Visible light driven photooxidation of phenol on TiO_2/Cu-loaded carbon catalysts

Marta A. Andrade[1,2], Rocio J. Carmona[2], Ana S. Mestre[1], Juan Matos[3], Ana P. Carvalho[1*], Conchi O. Ania[2*]

[1] Dpt. Química e Bioquímica and CQB, Faculdade de Ciências da Universidade de Lisboa, Ed. C8, Campo Grande 1749-016 Lisboa, Portugal

[2] Adsorption and Environmental Remediation on Porous Solids (ADPOR), Dpt. Chemical Processes for Energy and Environment, Instituto Nacional del Carbón, INCAR-CSIC, Apdo. 73, 33080 Oviedo, Spain

[3] Dpt. Photocatalysis and Alternative Energies, Venezuelan Institute for Scientific Research (IVIC), 20632, Caracas 1020-A, Venezuela

Abstract

The photocatalytic performance of titania/Cu-carbon composites was investigated towards phenol degradation under visible light. The approach consisted on the incorporation of the transition metal on the carbon component of the hybrid composite via impregnation of the carbon precursor with a metal salt followed by activation. Data showed a homogeneous dispersion of copper particles within the carbonaceous matrix, predominantly as copper (II) species. The synthesized carbons displayed a well developed nanoporous texture, although comparatively the impregnation of copper caused a marked inhibition of the textural development of the carbon precursor. The phenol photooxidation tests carried out on 1:1 titania/carbon composites showed the outstanding role of copper under visible light, with an increased efficiency in terms of phenol conversion, mineralization degree and degradation rate. This is important, since similar overall conversions were obtained with half of the amount of the photoactive semiconductor (1:1 composites). The beneficial effect of copper loading was also observed in the marked regioselectivity towards the preferential formation of catechol. Furthermore, the copper-loaded photocatalyst was found to be stable with no lixiviation or photorreduction of the copper species after illumination.

*Corresponding author. Tel./Fax: +353217500897/ +34 985 118846.

E-mail address: apcarvalho@fc.ul.pt (AP Carvalho) conchi.ania@incar.csic.es (CO Ania)

1. Introduction

In the last few years, a considerable amount of research has been carried out in the field of advanced oxidation processes (AOPs) to be applied in the removal and degradation of emergent contaminants from wastewaters [1-3]. Heterogeneous photocatalysis is widely recognized as an effective AOP for the degradation and mineralization of recalcitrant organic compounds [4-6]. Compared to other semiconductors, titanium dioxide plays a leading role as photocatalyst due to its costly effectiveness, low toxicity and high chemical photostability. As many other materials, titania powders suffer from several drawbacks mainly related to the low surface area, low activity under visible light, high recombination rate of photogenerated electron–hole pairs, and recovery and reutilization issues [7, 8]. Hence, many research efforts are being made to overcome these limitations. The incorporation of a carbon component as additive to semiconductors seems to be an adequate strategy to improve the efficiency of the photocatalyst; the enhanced performance of carbon/TiO_2 composites has been reported for the photodegradation of a variety of pollutants, and being attributed to several factors associated to visible light absorption, the porosity of the carbon support, strong interfacial electronic effects, and the intrinsic photochemical activity of certain carbons [9-12].

The incorporation of transition metals to improve the photocatalytic activity of TiO_2 has also been extensively investigated, with reported visible light activation of the doped photocatalyst due to the effective electronic interaction between the semiconductor and the metal [13-16]. Among transition metals, copper is a relatively available and effective dopant for trapping the electrons in the conduction band of TiO_2 [17-19]; additionally, many oxidative reactions are catalyzed by different copper complexes and oxides [20-22]. However, metal-doped semiconductors suffer from deactivation due to aggregation of the metallic dopants [23]. On the other hand, the incorporation of transition metals in the surface of carbonaceous materials appears as a powerful alternative offering great possibilities for the preparation of more efficient photocatalysts [24, 25], since the dispersion of metallic species on a carbonaceous matrix can be easily accomplished (by the choice of the precursor, and impregnation with metal oxides or salts) [26-31].

Knowing this, we aimed at exploring the photooxidative activity of copper-based materials by producing a hybrid titania/carbon photocatalyst incorporating copper on the carbon component during the carbon preparation step. The objective of this work is to study the photocatalytic activity of a Cu-loaded carbon/TiO_2 composite towards phenol degradation under visible light irradiation. As carbon component in the composite we have selected a nanoporous carbon prepared by chemical activation of a lignocellulosic precursor (sisal fibers,

discarded from the rope industry), in line with a current interest of our research group on the valorization of several types of residues for the production of low-cost adsorbents [32, 33]. Phenol was selected as model refractory contaminant, since it is a priority pollutant frequently found in wastewaters, representing a high environmental risk according to the European and American Environmental Protection Agencies.

2. Experimental

2.1 Materials synthesis

A copper-loaded nanoporous carbon was synthesized by chemical activation of a lignocellulosic industrial residue -discarded sisal ropes- supplied by a rope industry. Briefly, 1 cm long sisal pieces were impregnated with an aqueous solution of $Cu(NO_3)_2.3H_2O$ (Sigma-Aldrich, 99 %), with a concentration adjusted to attain 5 wt.% of copper in the final material, stirred overnight and dried. The material was then impregnated with a K_2CO_3 solution (Aldrich, 99 %), according to the weight ratio sisal: K_2CO_3 of 2:1, and activated in a horizontal furnace (Thermolyne Model 21100) at 700 ºC for 1 h under N_2 flow (5 cm^3 s^{-1}). After the activation, the sample was thoroughly washed with distilled water until pH 7 and dried at 100 ºC. This material will be referred to as SCu5. A blank sample was also prepared by activation with K_2CO_3 in the absence of copper (sample S). The titania/carbon photocatalysts with a 1:1 weight ratio composition were prepared by physical mixture of the individual components.

2.2 Characterization of the catalysts

The porosity of the samples was characterized by measuring the N_2 and CO_2 adsorption isotherms at -196 and 0 ºC, respectively (ASAP 2010 and Tristar 3020, Micromeritics). Before the experiments, the samples were outgassed under vacuum (ca. 10^{-3} torr) at 120 °C overnight. The isotherms were used to calculate the specific surface area, A_{BET}, total pore volume, V_{total}, while the micropore volumes were analyzed using the Dubinin–Radushkevich formulism to the N_2 and CO_2 adsorption data ($W_{0,N2}$, $W_{0,CO2}$) [34]. Elemental analysis was carried out in LECO CHNS-932 and LECO VTF-900 automatic analyzers. The surface chemistry was characterized by the determination of the pH at the point of zero charge (pH_{PZC}) using the mass-titration procedure, according to the experimental procedure described elsewhere [35]. The morphology of the samples and the dispersion of the metallic particles were observed by Field Emission Gun Scanning Electron Microscopy (FEG–SEM) with an X-ray Energy-Dispersive System (EDS) and Transmission Electron Microscopy

(TEM), in a JEOL JSM-7001F (using an accelerating voltage of 25 kV) and a Hitachi H-8100 (operating at 200 kV) equipments, respectively.

The actual copper content of sample SCu5 was determined by Inductively Coupled Plasma-Optical Emission Spectrometry (ICP-OES, Perkin Elmer Optima 2000 DV). The chemical state of the copper species was also investigated by X-ray Photoelectron Spectroscopy (XPS), and Temperature Programmed Reduction (TPR). X-ray photoelectron spectra were recorded on a SPECS spectrometer with a Phoibos 100 hemispherical analyzer with a multichannel detector. The base pressure in the ultra high vacuum chamber was below 10^{-7} kPa. The X-ray radiation source was monochromatic AlKα (1486.74 eV) at 100 W X-ray power and anode voltage of 14 kV. The photo-excited electrons were analyzed in constant pass energy mode, using pass energy of 50 eV for the survey spectra and 10 eV for the high resolution core level spectra. During data processing of the XPS spectra, binding energy values were referenced to the C 1s peak at 284.6 eV [36]. The CasaXPS software package was used for acquisition and data analysis. A Shirley-type background was subtracted from the signals. Recorded spectra were always fitted using Gauss–Lorentz curves, in order to determine the binding energy of the different element core levels more accurately. The error in binding energy was estimated to be ca. 0.1 eV. Photorreduction of Cu(II) species was avoided as much as possible by using short irradiation times (first acquisition was performed within 8 min), although reduction in high vacuum during the analysis cannot be excluded [37]. TPR analyses were performed in a chemisorption analyzer (Autochem 2920, Micromeritics) equipped with a TCD reactor and a mass spectrometer (OmniStar 3000). For each analysis approximately 40 mg of sample was treated with a 50 cm^3 min^{-1} stream of 10 % H_2 in Argon from 100 to 600 ºC at 5 ºC min^{-1}. X-ray diffraction (XRD) patterns were obtained at room temperature on a Philips PX-1730 with automatic data acquisition (APD Phillips (v3.6B) software), using CuKα radiation as incident beam.

2.3 Photodegradation runs

Phenol photodegradation experiments using commercially available titania (P25, Evonik) and titania/carbon composites - using a 1:1 weight ratio- as catalysts were carried out at room temperature using a photo-reactor of 500 cm^3 capacity, a loading catalyst ratio of 0.5 g L^{-1} and 85 ppm as initial phenol concentration in solution. The irradiation source was provided by a high pressure mercury lamp (Helios Italquartz, 125 W, emitting at 313, 360, 404, 436, 546, 577 and 579 nm; see spectrum in Supp. File), vertically suspended in a cylindrical, double-walled Pyrex jacket cooled by flowing water, immersed in the solution. The Pyrex jacket acts

as a cut-off filter of the UV irradiation lower than 360 nm, minimizing the photolytic reaction in all the catalytic runs. The water cell was used to control the temperature during the experiments, preventing any overheating of the suspension due to the irradiation. The reactor was open to air in all the experiments to ensure that enough oxygen was present in the reaction solution. In each run, 250 mg of the catalysts were added to 500 cm^3 of phenol solution under vigorous stirring (900 rpm). As we are studying porous photocatalysts, to maintain the same phenol concentration in solution (ca. 85 ppm) at the beginning of the irradiation, a pre-equilibration step at dark conditions was carried out to account for the amount adsorbed. Hence phenol adsorption kinetics of the materials was initially evaluated at dark conditions to establish the time required for the equilibrium (ca. 30 min in all cases) and the amount adsorbed. Consequently, before the irradiation was applied the composites were allowed to pre-equilibrate with phenol solutions of 95 and 105 ppm concentration, for TiO_2/S and TiO_2/SCu5 respectively. After the equilibration step, the suspension was irradiated for 360 min. All the experiments were done in duplicate with deviations below 5 % in all cases; reported data represent the average values.

During the irradiation, small aliquots of the solution (~ 1 cm^3) were taken out at predetermined time intervals and analyzed by reverse-phase HPLC (Spherisorb C18 column 125 mm x 4 mm, methanol to water 5:95, 30 ºC, 0.7 cm^3 min^{-1} flow rate, photodiode array detector). The samples were previously filtered using cellulose filters having mean pore size of 0.45 μm. Total organic carbon (TOC) of the solution at the end of each run was also measured in a TOC-V analyzer.

Assays in the same experimental conditions, but in the absence of irradiation, were performed (series *dark*) for further comparison with the experiments upon irradiation (series *irrad*) of the catalysts, so as to detect any modifications upon illumination. The spent catalysts were recovered by filtration, dried overnight at 60 ºC and characterized. An aqueous suspension of the Cu-loaded carbon was also irradiated to investigate the possible photo-induced degradation of the carbonaceous matrix. The concentration of copper ions potentially released to the solution during the photocatalytic experiments was monitored by ICP-MS (Agilent).

3. Results and discussion

3.1 *Characterization of the materials*

A detailed textural characterization of the nanoporous carbons and the TiO_2/carbon composites as well as that of P25 is summarized in Fig. 1(a-c) and Table 1. The carbon samples prepared by chemical activation of the sisal waste resulted to be essentially

microporous materials. Comparatively, the impregnation with copper of the carbon precursor resulted in the inhibition of the textural development, as revealed by the pronounced drop in the apparent surface area (larger than 30 %), that goes beyond the mass effect of copper (ca. 5 wt. %). Furthermore, for the copper-loaded samples (both SCu5 and TiO_2/SCu5), $W_{0,N2} < W_{0,CO2}$, which is indicative of a narrow microporous distribution as opposed to the non-loaded materials (with $W_{0,N2} > W_{0,CO2}$) [38] . This micropore distribution is attributed to the porosity of the carbon component, since TiO_2 is non-porous. The evaluation of the micropore size distribution from the CO_2 adsorption isotherms at 0 ºC (Fig. 1 (d)) [39] confirmed the broader distribution of micropores in the raw activated carbon, with a maximum centered at the same value (ca. 0.5 nm) for both carbons but extended to micropores of larger size for the non copper loaded carbon.

For the TiO_2/carbon composites, the nitrogen adsorption isotherms changed towards a hybrid I/IV shape, confirming that they inherited the textural properties of both precursors according to expectations. A large decrease in the apparent surface area and microporosity (roughly 50 %) was also observed for the composites. This result was rather expected for 1:1 composites, due to the non-porous nature of P25, with a low specific surface area and a type II nitrogen adsorption isotherm, Fig. 1(c).

Table 1. Main textural parameters of the investigated materials obtained from gas adsorption, data.

Sample	A_{BET} ($m^2 g^{-1}$)	V_{total}[1] ($cm^3 g^{-1}$)	V_{meso}[2] ($cm^3 g^{-1}$)	$W_{0,N2}$ ($cm^3 g^{-1}$)	$W_{0,CO2}$ ($cm^3 g^{-1}$)
TiO_2	57	0.14	--	0.02	-
S	968	0.45	0.04	0.41	0.37
TiO_2/S	484	0.23	0.02	0.21	0.15
TiO_2/S *dark*	236	0.13	0.02	0.11	-
TiO_2/S *irrad*	288	0.16	0.04	0.12	0.14
SCu5	674	0.31	0.01	0.30	0.34
TiO_2/SCu5	292	0.17	0.04	0.13	0.23
TiO_2/SCu5 *dark*	190	0.12	0.03	0.09	-
TiO_2/SCu5 *irrad*	201	0.13	0.04	0.09	0.12

[1] Evaluated at $p/p^0 = 0.9$, to avoid the contribution of the inter particular voids in P25 and in the composites; [2] Difference between V_{total} and $W_{0,N2}$.

As for the nature of the carbons, the elemental analysis and their pH_{PZC} values are displayed on Table 2. Both carbons present rather large oxygen contents, a usual characteristic of lignocellulosic materials [40] , which is also in agreement with the slightly acidic nature of both materials, as evaluated by the pH_{PZC} values.

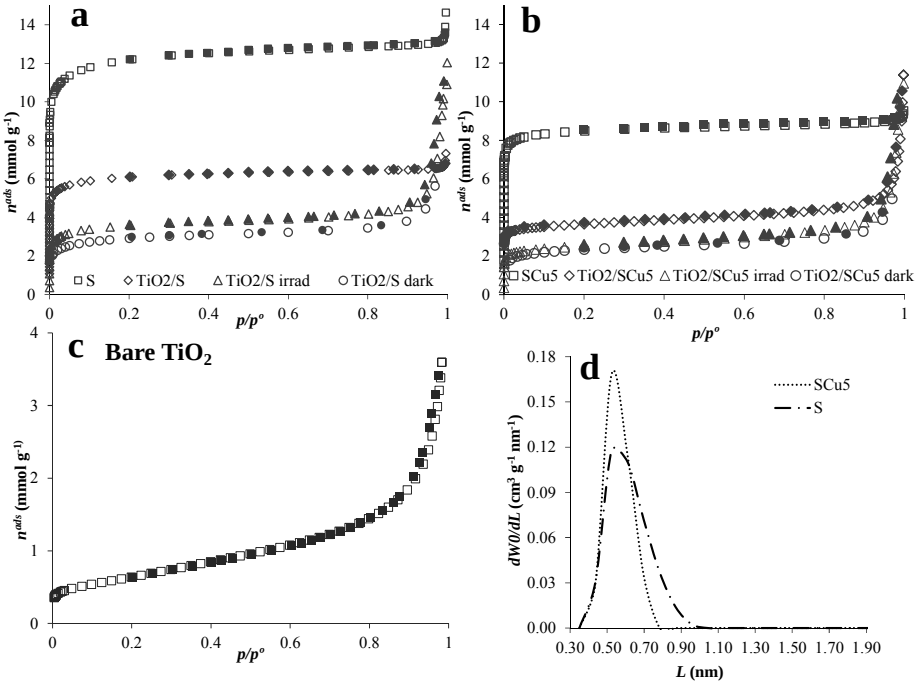

Fig. 1- (a, b, c) Nitrogen adsorption-desorption isotherms at -196 ºC (closed symbols are desorption points); (d) Micropore size distributions obtained from the CO_2 adsorption data according to the method described in Pinto et al [39].

Table 2. Elemental analysis (wt.%) and pH of the point of zero charge of the studied carbon materials. For a better comparison of the samples, the composition is shown on a dry basis.

Elemental analysis (wt. %)							pH_{PZC}
	C	H	N	S	O	ash	
S	80.3	1.2	0.2	0.01	15.4	3.1	5.3
SCu5	75.1	1.0	0.5	0	15.0	8.5	6.0

The analysis of the composition of sample SCu5 revealed 4.8 wt.% of copper content, as expected based on the synthesis procedure followed. The SEM and TEM images (Fig. 2) showed a good dispersion of the metallic particles of different sizes along the carbon matrix,

with no visual signs of copper clustering in large metallic aggregates; the homogeneous distribution of small copper particles was also supported by the EDX mapping.

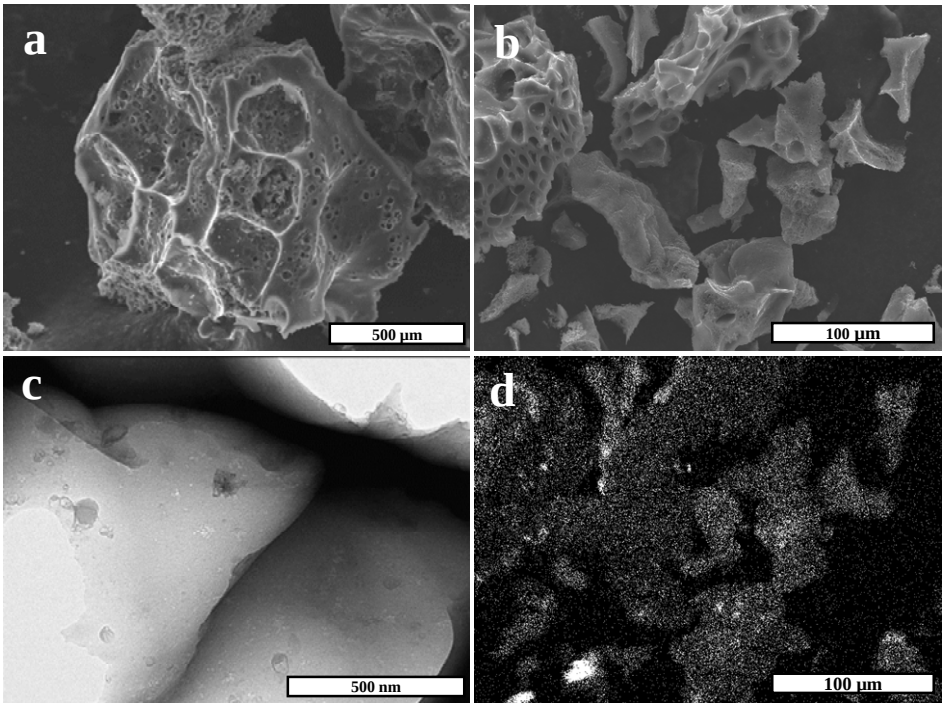

Fig. 2. SEM images of the unloaded (a) and copper loaded (b) carbons; (c) TEM image and (d) EDX mapping of Cu for SCu5.

The chemical state and distribution of copper species in the carbon matrix was investigated by XRD and XPS (Fig. 3 and 4). The XRD patterns of SCu5 were analyzed according to the International Center for Diffraction Data (ICDD) and revealed the presence of Cu^0 (ICDD 4-836), Cu_2O (ICDD 5-0667) and CuO (ICDD 5-0661) species. Regarding the XPS analysis, the Cu 2p core level spectra of SCu5 showed the main Cu $p_{3/2}$ signal, composed of two contributions at 932.5 and 934.5 eV that are assigned to surface Cu(I) and Cu(II), with fractions of 14 and 85 %, respectively. The high ratio of the areas of the satellite region (938-945 eV) and the area of the main Cu $2p_{3/2}$ signal indicates that oxidized copper species are predominant (value Cu $2p_{3/2}$sat/Cu $2p_{3/2}$mp of 0.46, whereas when only Cu(II) species are present this ratio is 0.55). The small signal at 932.9 eV (accounting for only 0.7%) suggests that the surface contribution of reduced copper is almost negligible despite it was detected by XRD. This suggests that Cu^0 is located in the inner surface of the carbon, rather than in the external area.

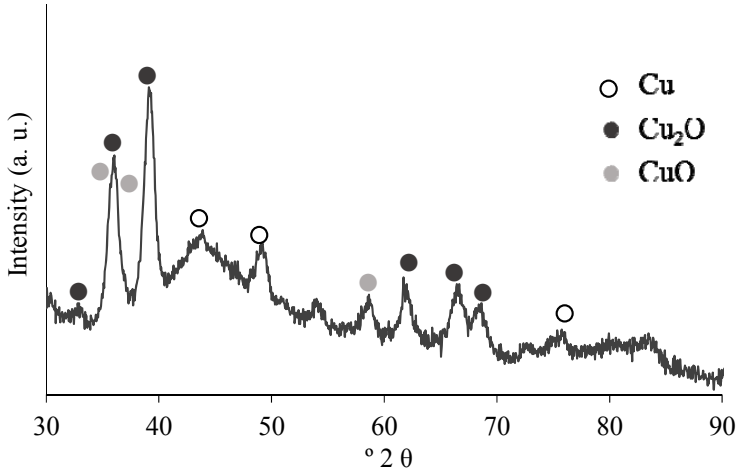

Fig. 3. X-ray diffraction pattern of the copper-loaded carbon (sample SCu5).

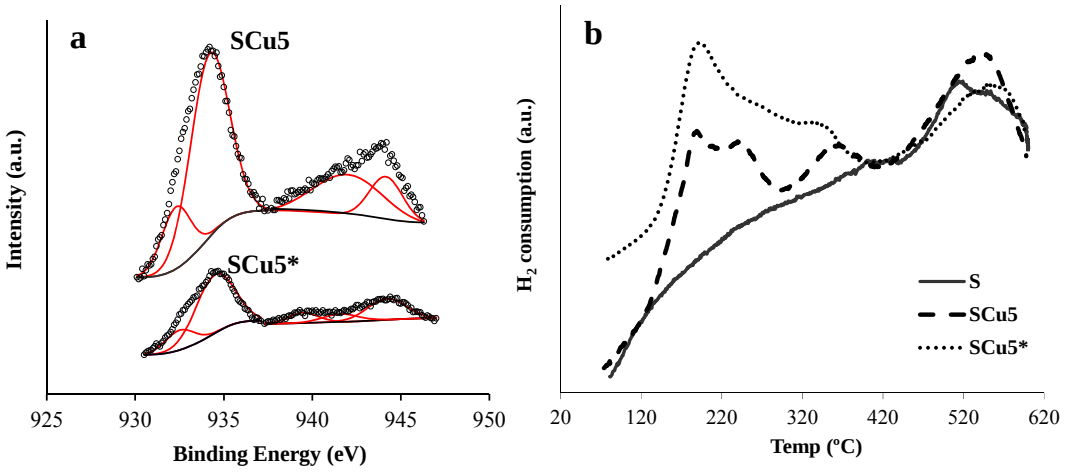

Fig. 4. (a) Cu $2p_{3/2}$ XPS spectrum for sample SCu5 and the sample obtained after illumination in aqueous solution, SCu5*; (b) TPR for samples S and SCu5 and the sample obtained after illumination in aqueous solution, SCu5*.

TPR data shown in Fig. 4 also point out to a large contribution of Cu(II) and Cu(I) species. The profiles show two clearly distinguished areas, with decomposition peaks due to the reduction of copper in the range of 150 – 400 ºC; the hump at higher temperatures (above 400 ºC) are attributed to the reduction of oxygen species of the carbon, as they also appear in the unmodified carbon [41]. Deconvolution of TPR plots was performed using Gaussian curves to facilitate data interpretation. Three reduction peaks are presented at 190, 245 and 360 ºC, that are assigned to the stepwise reduction of copper oxide ($Cu^{2+} \rightarrow Cu^{+} \rightarrow Cu^{0}$), [42,

43]. The reduction of bulk CuO is considered as one-step process at about 230 ^{o}C [44], while multistep patterns have been reported for supported CuO. The lower temperature of the reduction profile of SCu5 implies that the metallic species are small and highly dispersed in the carbon matrix [45, 46].

3.2 *Photocatalytic experiments*

Due to the porous nature of the carbon materials a pre-equilibration step at dark conditions was carried out before the photocatalytic runs, to assure the same phenol concentration in solution at the beginning of the illumination for all three studied materials. This approach allowed the discrimination of the fraction of degraded pollutant in the photocatalytic reaction from that removed by adsorption -an important issue in porous catalysts. Furthermore, the use of a Pyrex filter to cut-off the UV contribution of the irradiation source also allowed to neglect the effect of direct photolysis (Fig. 5), whose contribution can be expected due to the changes in the solution concentration [47].

Hence, phenol adsorption kinetics and capacity of both S and SCu5 carbons were previously evaluated at dark conditions. The initial rate of phenol adsorption was very fast for both cases with the equilibrium uptake attained after 30 min. This is consistent with their well developed porosity, as shown in Table 1. For bare titania, the amount of phenol adsorbed at dark conditions is almost negligible (~3 %), as expected given its non-porous nature. Consequently the initial phenol concentration in solution was adjusted for S and SCu5 (95 and 105 ppm, respectively), to achieve 85 ppm after the preequilibration step. Additionally, irradiation of aqueous suspensions of the carbon materials confirmed their stability under our illumination conditions, as neither the carbonaceous matrix nor copper species on the metal-loaded carbon lixiviated. The lack of copper ions release to the solution is reasonable considering that the solution pH did not significantly change during the photocatalytic runs (ranging from 6.5 to 4.9).

The photocatalytic behavior of the studied catalysts under visible light is presented in Fig. 5. As stated before, under our experimental conditions the effect of direct photolysis can be neglected (phenol conversion after 6 hours of irradiation was below 3 % with no noticeable mineralization), while adsorption is suppressed in the pre-equilibration step; thus conversion can be exclusively ascribed to the photocatalytic efficiency of the studied materials. Several differences become clear when comparing the performance of the TiO_2/carbon composites to that of bare titania. First of all, phenol removal efficiency was slightly better for the composites, with values of 57, 62 and 73 % after 6 h of irradiation, for TiO_2, TiO_2/S and

TiO_2/SCu5, respectively. Although the conversion values may seem somewhat low for titania-based photocatalysts, it should be recalled that only visible light is used in this work (see experimental section). What is interesting to note is that phenol photooxidation efficiency was significantly enhanced for the TiO_2/carbon composites, when compared to that of TiO_2 alone. This is particularly observed for the copper-loaded carbon, which also rendered a better photocatalytic response than the composite based on the unmodified carbon.

To compare the photocatalytic activity of the studied materials, the kinetic curves in Fig. 5 were fitted to the Langmuir-Hinshelwood model using the simplified apparent first-order equation (Table 3). The first-order apparent rate constants followed the trend: $TiO_2 < TiO_2/S < TiO_2/SCu5$, with the latter presenting a rate constant 1.6 and 1.2 times higher than TiO_2 and composite TiO_2/S, respectively. This data shows the cooperative effect between the carbon and the inorganic component of the catalysts, as well as the copper effect on accelerating the photooxidation reaction under visible light.

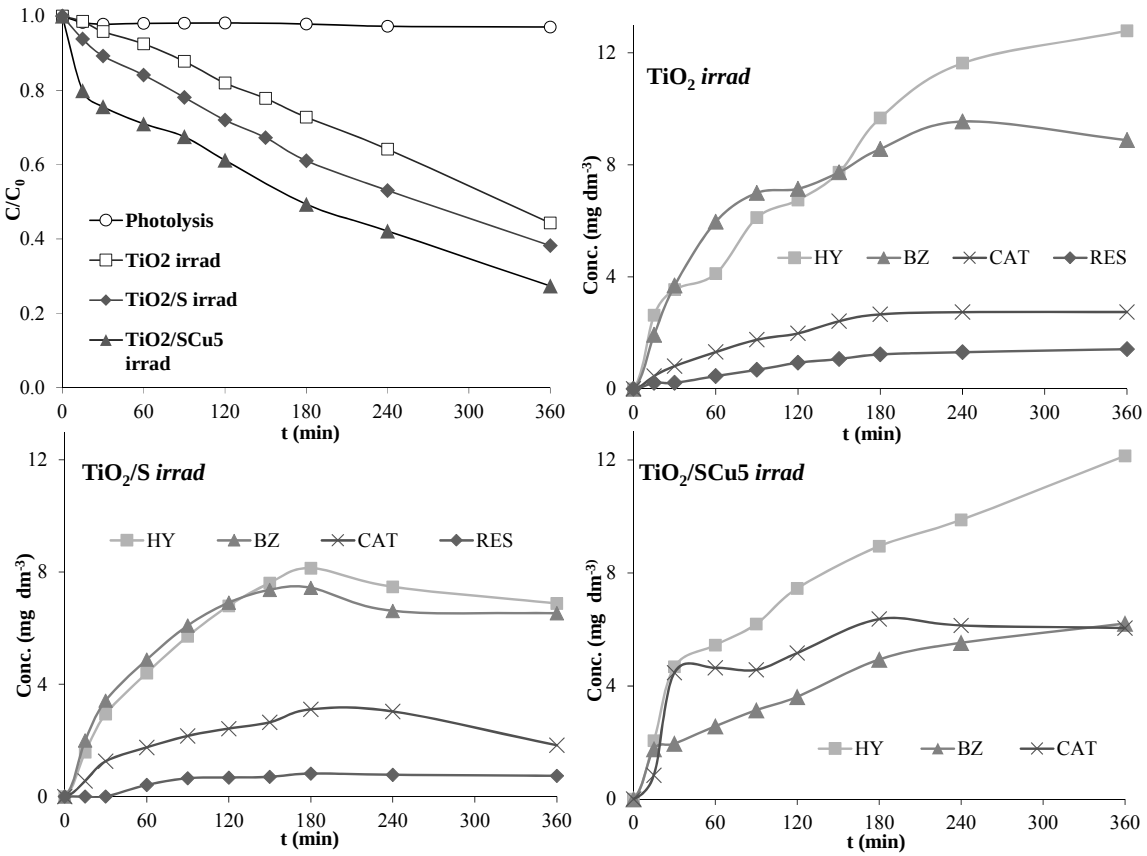

Fig. 5. (a) Phenol concentration decay curves of the investigated materials under irradiation. (b, c, d) Evolution of phenol degradation intermediates detected upon irradiation of the materials investigated (HY- hydroquinone; BZ- benzoquinone; CAT-catechol, RES-resorcinol).

Table 3- Apparent first-order rate constants (k_{app}), half reaction time ($t^{1/2}$) and correlation coefficient (R^2) obtained from fitting experimental data to the Langmuir–Hinshelwood model ($\ln (C_0/C) = k_{app}\, t$).

Sample	$k_{app} \times 10^{-3}$ (min^{-1})	$t_{1/2}$ (min)	R^2
TiO_2 *irrad*	1.9	365	0.994
TiO_2/S *irrad*	2.6	267	0.999
TiO_2/SCu5 *irrad*	3.1	224	0.993

Secondly, although the detected intermediate products were the same for all three studied catalysts, their amount and distribution was different (Fig. 5), with slightly higher values for bare titania than for TiO_2/carbon composites. Phenol degradation pathway using TiO_2 and TiO_2/S was similar, with quinones (hydroquinone and benzoquinone) as predominant intermediates and concentrations reaching a maximum after ca. 3 h of irradiation. In the case of TiO_2/SCu5, a marked regioselectivity is noticed towards the preferential oxidation in ortho position to form catechol. Such regioselective formation of catechol over quinones has been reported for other carbon materials under UV illumination [12] and copper catalysts in wet oxidation reactions [48] and it is considered more advantageous for the overall reaction yield, due to the higher reactivity of catechols over quinones [49, 50]. Given the less energetic irradiation source used in this work, we attribute this characteristic to the copper loading, although the contribution of the carbon matrix cannot be completely ruled out.

The mineralization degree was estimated from the total organic carbon values determined in solution after 6 hours of irradiation (Table 4) and considering an initial TOC value of 65 mg C L^{-1}, that corresponds to the concentration of phenol in solution after the pre-equilibration step. The highest mineralization degree after 6 hours of irradiation was obtained for the copper-loaded carbon composite (ca. 42 %), almost twice as larger than that of titania and the unmodified carbon composite. This demonstrates that the effect of copper does not only enhance the photooxidation rate (Table 3) and modifies the degradation pathway (Fig. 5) but also shows a superior photocatalytic activity under visible light.

On the other hand, similar mineralization values were obtained for bare titania and TiO_2/S composite. These are interesting results bearing in mind that, as the experiments were carried out with a constant total solid loading of 0.5 g L^{-1}, the amount of semiconductor on the composites (ratio 1:1) is half of the amount used in the experiments with titania powders.

Furthermore, the conversion obtained using titania with a total solid loading of 0.25 g L^{-1} (the same as in the composites) was below 40%.

The difference between the values of TOC and the TOC_{HPLC}, computed considering the aromatic intermediates detected by HPLC (Table 4) can give us an indication of the amount of short-chain alkyl acids present in solution at the end of the reaction. In fact, the smaller difference between these values, that is, the lesser amount of acids, is observed for composite TiO_2/SCu5, which is in good agreement with the high mineralization value obtained, and points out the positive effect of copper towards an efficient photooxidation of phenol itself and its degradation products.

Table 4. Total Organic Carbon (TOC, mg C L^{-1}) values and mineralization degree after 6 hours irradiation of the catalysts. Initial TOC value was 65 mg C L^{-1} for all the samples.

Sample	TOC (t=360 min)	TOC_{HPLC} [1] (phenol+TQ+CAT+RES)	Mineralization %
TiO_2 *irrad*	55.3	48.3	27
TiO_2/S *irrad*	50.4	40.3	20
TiO_2/SCu5 *irrad*	37.5	32.3	42

According to the literature, copper catalysts may suffer deactivation during oxidation reactions caused by the leaching of the copper cation under specific conditions (temperature, pH), with important consequences on the toxicity of the effluents due to the change from heterogeneous to homogeneous catalysis [51]. Hence, the spent catalysts were analyzed to detect any likely modifications in the course of the photocatalytic runs. XPS data in Fig. 4(a) shows that the chemical status of the copper species in SCu5 was not modified after irradiation in aqueous solution (SCu5*). The patterns showed the negligible contribution of Cu(0) at 932.9 eV and a similar ratio of the areas of the main peaks and the satellite regions (ratio Cu $2p_{3/2}$sat/Cu $2p_{3/2}$mp of 0.49). However, some changes appeared on the TPR profiles of sample SCu5*, Fig. 4(b). Although the patterns exhibit a similar stepwise reduction fingerprint of copper oxide, the deconvolution of the peaks showed a slight decrease (ca. 20 %) in the contribution of the peak at 190 ºC -assigned to the presence of oxocations $(Cu\text{-}O\text{-}Cu)^{2+}$-, at expenses of the contribution at 245 ºC, ascribed to copper oxide particles of larger sizes or to copper oxide species with lower oxidation states [42, 43]. This suggests a

slight photorreduction of the copper (II) species, or an agglomeration of the dispersed metallic particles. Anyhow, this is not observed on the surface of the catalysts (XPS data) nor in solution (no lixiviation of copper), indicating that the changes occur in the bulk of the catalysts.

The analysis of the textural properties of the composites after irradiation (series *irrad)* and after adsorption in the absence of irradiation (series *dark*) provides an interesting insight on the photooxidation process on porous catalysts. As seen in Table 1, the porosity of the series *irrad* and *dark* was similar, indicating a similar fraction of species adsorbed for both cases and hence suggesting that further adsorption of phenol and/or degradation intermediates in the course of the photooxidation experiments can be discarded. Also, although the porosity of the carbon is partially clogged in both cases, the composites still present relatively large pore volumes and surface areas (a significant fraction of the porosity remains unoccupied).

Summarizing, our data shows the positive effect of copper loading of the carbon component on phenol photooxidation reaction, in terms of phenol conversion, regioselectivity in the formation of intermediates, superior mineralization degree and enhanced degradation rate. To analyze the effect of copper, several aspects have to be considered.

First of all, based on the synthesis procedure of the copper-loaded carbons, we do not expect any modification of the crystalline structure of the semiconductor as the metallic species are dispersed in the carbon matrix. Indeed, the optical properties of the TiO_2/carbon composites (Fig S1 in Supplementary Information) showed the characteristic absorption sharp edge of the anatase form of TiO_2 (predominant phase) in the UV region lying above 400 nm, and the broader background absorption in the visible light region due the to the presence of the carbon component. The absorption onset was about the same for all three studied catalysts, with no differences for the Cu-loaded and unmodified carbon composites, as expected considering the low copper loading (i.e., 5 wt.%).

On the other hand, copper could act as an oxygen activator. The carbonaceous phase with well dispersed copper species is expected to create a specific fast electron transfer environment (which would minimize the recombination of the excited electron/hole pairs created upon illumination of the semiconductor), as well as specific hydrophobic sites on which molecular oxygen dissolved in water is easily adsorbed (the higher hydrophobicity of the Cu-loaded carbon is confirmed by the pH_{PZC} and water adsorption experiments, see SI). This would also favor the formation of O-radical species -promoted by the reaction with the photogenerated charge carriers- that would contribute to the enhanced photooxidation reaction. In this regard, several studies in the literature have reported that some copper-organic complex (porphyrins,

phthalocyanines) have strong absorption in the visible light region and can activate O_2 or H_2O_2 to oxidize toxic organic pollutants [52-54], mimicking the activity of peroxidases [55]. Our material could follow a similar mechanism as that proposed for copper catalysts in wet oxidation reactions [56-58], initiated by the light absorption of the semiconductor. The photoexcitation of the semiconductor near the Cu(II) species can lead to the subsequent formation of O-radicals under visible light irradiation, to produce Cu+ intermediates. The reduced metal species have high electronegativity, and thus interact with dissolved O_2 (retained in the nanoporosity of the carbon component), to regenerate the Cu(II) and further radical species responsible for the improved phenol photooxidation.

Further studies with spectroscopic tools are currently ongoing to provide experimental evidences on the formation of the radicals, expected based on the quantification of the degradation intermediates and the superior performance of the Cu-loaded carbon/TiO_2 composite in the overall phenol conversion and mineralization extent.

4. Conclusions

This work investigated the photocatalytic performance of a copper-containing photocatalyst composite towards phenol degradation using visible light. The incorporation of the transition metal was carried out on the carbon component of the hybrid composite, by impregnation of the carbon precursor with a copper salt and subsequent chemical activation. The copper-loaded carbon displayed a well developed porosity and a good dispersion of metallic particles within the carbonaceous matrix. The analysis of the chemical status of the metal showed that oxidized copper species are dominant in the prepared material, as expected by the oxidizing atmosphere during the activation.

The performance of the synthesized titania/carbon composites for the photodegradation of phenol under visible light has been evaluated and compared to that of commercial TiO_2 under similar experimental conditions. The enhanced overall efficiency in terms of phenol conversion, mineralization degree and degradation rate found for the copper-loaded hybrid composite, showed the outstanding role of copper incorporated on the carbon matrix. This is important since the amount of semiconductor in the composites (ratio 1:1) is half of the amount used in the experiments with titania powders. The analysis of the textural properties of the composites after irradiation showed an interesting insight on the photooxidation process. A similar clogging of the porosity of the photocatalysts was found in dark and irradiation conditions, demonstrating that the higher conversion values cannot be solely attributed to the adsorption.

The beneficial effect of copper loading was also observed in the marked regioselectivity towards the preferential formation of catechol over quinones, which is considered to be more effective for a complete mineralization. Furthermore, the copper-loaded photocatalyst was found to be stable with no lixiviation or photorreduction of the copper species after illumination. As the optical properties of the photoactive semiconductor were not modified upon the incorporation of the copper species on the carbon component, the effect of copper is attributed to several factors including its role as oxygen activator and/or the fast electron transfer environment, which would minimize the recombination of the excited electron/hole pairs created upon illumination of the semiconductor.

Although further studies with spectroscopic tools are needed to confirm the role of copper on the superior performance of the TiO_2/Cu-carbon composite, several hypotheses may be postulated. The photooxidation reaction would be initiated by the light absorption of the semiconductor near the Cu(II) species, and leading to the formation of O-radicals under visible light irradiation. The reduced metal species would interact with dissolved O_2 adsorbed in the hydrophobic sites of the carbon component, thereby regenerating the Cu(II) and further radical species responsible for the improved phenol photooxidation.

ACKNOWLEDGMENTS

The authors thank Cordex (Portugal) for kindly supplying sisal. The financial support of the pluriannual funding to CQB (PEst-OE/QUI/UI0612/2013), MINECO (CTM2008/01956, CTM2011/23378, AIB2010-PT00209) and PCTI Asturias (Fondos Feder 2007-2013, grant PC10-002) is also acknowledged. MAA and ASM thank FCT for their PhD (SFRH/BD/71673/2010) and postdoc (SFRH/BPD/86693/2012) fellowships, respectively. RJC thanks PCTI Asturias for her Severo Ochoa fellowship.

References

[1] Oppenlander T. Photochemical purification of water and air: advanced oxidation processes (AOPs): Principles, reaction mechanisms, reactor concepts.: Wiley-VHC; 2003.

[2] Comninellis C, Kapalka A, Malato S, Parsons SA, Poulios L, Mantzavinos D. Advanced oxidation processes for water treatment: advances and trends for R&D. J Chem Technol Biot. 2008;83(6):769-76.

[3] Gogate PR, Pandit AB. A review of imperative technologies for wastewater treatment I: oxidation technologies at ambient conditions. Adv Environ Res. 2004;8(3-4):501-51.

[4] Ollis DF, Al-Ekabi H. Photocatalytic purification and treatment of water and air. Amsterdam: Elsevier; 1993.

[5] Pelizzetti E, Serpone N. Photocatalysis: fundamentals and applications. New York: Wiley; 1989.

[6] Legrini O, Oliveros E, Braun AM. Photochemical processes for water treatment. Chem Rev. 1993;93(2):671-98.
[7] Fujishima A, Zhang XT, Tryk DA. TiO_2 photocatalysis and related surface phenomena. Surf Sci Rep. 2008;63(12):515-82.
[8] Hashimoto K, Irie H, Fujishima A. TiO2 photocatalysis: A historical overview and future prospects. Jpn J Appl Phys 1. 2005;44(12):8269-85.
[9] Leary R, Westwood A. Carbonaceous nanomaterials for the enhancement of TiO_2 photocatalysis. Carbon. 2011;49(3):741-72.
[10] Matos J, Garcia A, Zhao L, Titirici MM. Solvothermal carbon-doped TiO_2 photocatalyst for the enhanced methylene blue degradation under visible light. Appl Catal A: Gen. 2010;390(1-2):175-82.
[11] Bandosz TJ, Matos J, Seredych M, Islam MSZ, Alfano R. Photoactivity of S-doped nanoporous activated carbons: A new perspective for harvesting solar energy on carbon-based semiconductors. Appl Catal a-Gen. 2012;445:159-65.
[12] Velasco LF, Fonseca IM, Parra JB, Lima JC, Ania CO. Photochemical behaviour of activated carbons under UV irradiation. Carbon. 2012;50(1):249-58.
[13] Choi WY, Termin A, Hoffmann MR. The role of metal-ion dopants in quantum-sized TiO_2 - Correlation between photoreactivity and charge-carrier recombination dynamics. J Phys Chem-Us. 1994;98(51):13669-79.
[14] Inturi SNR, Boningari T, Suidan M, Smirniotis PG. Visible-light-induced photodegradation of gas phase acetonitrile using aerosol-made transition metal (V, Cr, Fe, Co, Mn, Mo, Ni, Cu, Y, Ce, and Zr) doped TiO_2. Appl Catal B:Environ. 2014;144:333-42.
[15] Rashad MM, Elsayed EM, Al-Kotb MS, Shalan AE. The structural, optical, magnetic and photocatalytic properties of transition metal ions doped TiO_2 nanoparticles. J Alloy Compd. 2013;581:71-8.
[16] Maicu M, Hidalgo MC, Colon G, Navio JA. Comparative study of the photodeposition of Pt, Au and Pd on pre-sulphated TiO_2 for the photocatalytic decomposition of phenol. J Photoch Photobio A. 2011;217(2-3):275-83.
[17] Colon G, Maicu M, Hidalgo MC, Navio JA. Cu-doped TiO_2 systems with improved photocatalytic activity. Appl Catal B:Environ. 2006;67(1-2):41-51.
[18] Xin BF, Wang P, Ding DD, Liu J, Ren ZY, Fu HG. Effect of surface species on Cu-TiO_2 photocatalytic activity. Appl Surf Sci. 2008;254(9):2569-74.
[19] Irie H, Kamiya K, Shibanuma T, Miura S, Tryk DA, Yokoyama T, et al. Visible light-sensitive Cu(II)-grafted TiO_2 photocatalysts: activities and X-ray absorption fine structure analyses. J Phys Chem C. 2009;113(24):10761-6.
[20] Kang P, Bobyr E, Dustman J, Hodgson KO, Hedman B, Solomon EI, et al. Bis(mu-oxo) dicopper(III) species of the simplest peralkylated diamine: enhanced reactivity toward exogenous substrates. Inorg Chem. 2010;49(23):11030-8.
[21] Chen ZF, Meyer TJ. Copper(II) catalysis of water oxidation. Angew Chem Int Edit. 2013;52(2):700-3.
[22] Chen ZF, Kang P, Zhang MT, Stoner BR, Meyer TJ. Cu(II)/Cu(0) electrocatalyzed CO_2 and H_2O splitting. Energ Environ Sci. 2013;6(3):813-7.
[23] Nishikiori H, Sato T, Kubota S, Tanaka N, Shimizu Y, Fujii T. Preparation of Cu-doped TiO_2 via refluxing of alkoxide solution and its photocatalytic properties. Res Chem Intermediat. 2012;38(2):595-613.
[24] Nguyen-Thanh D, Bandosz TJ. Metal-loaded carbonaceous adsorbents templated from porous clay heterostructures. Micropor Mesopor Mat. 2006;92(1-3):47-55.
[25] Ania CO, Bandosz TJ. Highly mesoporous carbons obtained using a dynamic template method. Micropor Mesopor Mat. 2006;89(1-3):315-24.

[26] Ania CO, Bandosz TJ. Metal-loaded polystyrene-based activated carbons as dibenzothiophene removal media via reactive adsorption. Carbon. 2006;44(12):2404-12.
[27] Petit C, Karwacki C, Peterson G, Bandosz TJ. Interactions of ammonia with the surface of microporous carbon impregnated with transition metal chlorides. J Phys Chem C. 2007;111(34):12705-14.
[28] Hines D, Bagreev A, Bandosz TJ. Surface properties of porous carbon obtained from polystyrene sulfonic acid-based organic salts. Langmuir. 2004;20(8):3388-97.
[29] Hermans S, Deffernez A, Devillers M. Preparation of Au-Pd/C catalysts by adsorption of metallic species in aqueous phase for selective oxidation. Catal Today. 2010;157(1-4):77-82.
[30] Alvarez-Montero MA, Gomez-Sainero LM, Mayoral A, Diaz I, Baker RT, Rodriguez JJ. Hydrodechlorination of chloromethanes with a highly stable Pt on activated carbon catalyst. J Catal. 2011;279(2):389-96.
[31] Qiu BA, Han LN, Wang JC, Chang LP, Bao WR. Preparation of sorbents loaded on activated carbon to remove H_2S from hot coal gas by supercritical water impregnation. Energ Fuel. 2011;25:591-5.
[32] Mestre AS, Bexiga AS, Proenca M, Andrade M, Pinto ML, Matos I, et al. Activated carbons from sisal waste by chemical activation with K_2CO_3: Kinetics of paracetamol and ibuprofen removal from aqueous solution. Bioresource Technol. 2011;102(17):8253-60.
[33] Cabrita I, Ruiz B, Mestre AS, Fonseca IM, Carvalho AP, Ania CO. Removal of an analgesic using activated carbons prepared from urban and industrial residues. Chem Eng J. 2010;163(3):249-55.
[34] Gregg SJ, Sing KSW. Adsorption, Surface Area and Porosity. 2nd ed. London: Academic Press Inc.
[35] Noh JS, Schwarz JA. Estimation of the Point of Zero Charge of Simple Oxides by Mass Titration. J Colloid Interf Sci. 1989;130(1):157-64.
[36] J.F. Moulder WFS, P.E. Sobol, K.D. Bomben. Standard spectra for identification and interpretation of XPS data. Eden Prairie, MN: Perkin Elmer.
[37] Poulston S, Parlett PM, Stone P, Bowker M. Surface oxidation and reduction of CuO and Cu_2O studied using XPS and XAES. Surf Interface Anal. 1996;24(12):811-20.
[38] Rodríguez-Reinoso F, Sepúlveda-Escribano A. Porous carbons in adsorption and catalysis. In: Nalwa HS, ed. Handbook of surfaces and interfaces of materials. London: Academic Press 2001, p. 309-55.
[39] Pinto ML, Mestre AS, Carvalho AP, Pires J. Comparison of methods to obtain micropore size distributions of carbonaceous materials from CO_2 adsorption based on the Dubinin-Radushkevich isotherm. Ind Eng Chem Res. 2010;49(10):4726-30.
[40] Andrade M, Parra JB, Haro M, Mestre AS, Carvalho AP, Ania CO. Characterization of the different fractions obtained from the pyrolysis of rope industry waste. J Anal Appl Pyrol. 2012;95:31-7.
[41] Barrabes N, Just J, Dafinov A, Medina F, Fierro JLG, Sueiras JE, et al. Catalytic reduction of nitrate on Pt-Cu and Pd-Cu on active carbon using continuous reactor - The effect of copper nanoparticles. Appl Catal B-Environ. 2006;62(1-2):77-85.
[42] Chen LY, Horiuchi T, Osaki T, Mori T. Catalytic selective reduction of NO with propylene over Cu-Al_2O_3 catalysts: influence of catalyst preparation method. Appl Catal B:Environ. 1999;23(4):259-69.
[43] Tsoncheva T, Linden A, Areva S, Minchev C. Copper oxide modified large pore ordered mesoporous silicas for ethyl acetate combustion. Catal Commun. 2006;7(6):357-61.
[44] Hartmann M, Racouchot S, Bischof C. Characterization of copper and zinc containing MCM-41 and MCM-48 mesoporous molecular sieves by temperature programmed reduction and carbon monoxide adsorption. Micropor Mesopor Mat. 1999;27(2-3):309-20.

[45] Subbaramaiah V, Srivastava VC, Mall ID. Catalytic activity of Cu/SBA-15 for peroxidation of pyridine bearing wastewater at atmospheric condition. Aiche J. 2013;59(7):2577-86.
[46] Bian J, Xiao M, Wang SJ, Lu YX, Meng YZ. Carbon nanotubes supported Cu-Ni bimetallic catalysts and their properties for the direct synthesis of dimethyl carbonate from methanol and carbon dioxide. Appl Surf Sci. 2009;255(16):7188-96.
[47] Priya SS, Premalatha, M, Subramanian, P. Elucidation of kinetics of photolysis of phenol. Journal of the Institution of Engineers: Chemical Engineering.90:10-6.
[48] Santos A, Yustos P, Quintanilla A, Garcia-Ochoa F. Kinetic model of wet oxidation of phenol at basic pH using a copper catalyst. Chem Eng Sci. 2005;60(17):4866-78.
[49] Santos A, Yustos P, Quintanilla A, Rodriguez S, Garcia-Ochoa F. Route of the catalytic oxidation of phenol in aqueous phase. Appl Catal B-Environ. 2002;39(2):97-113.
[50] Ross L BC, Vinqvist MR. Phenols as antioxidants. In: Rappoport Z, ed. The Chemistry of Phenols. England: John Wiley & Sons; 2003, p. p. 839-909.
[51] Santos A, Yustos P, Quintanilla A, Garcia-Ochoa F, Casas JA, Rodriguez JJ. Evolution of toxicity upon wet catalytic oxidation of phenol. Environ Sci Technol. 2004;38(1):133-8.
[52] Mohamed RM, Mohamed MM. Copper (II) phthalocyanines immobilized on alumina and encapsulated inside zeolite-X and their applications in photocatalytic degradation of cyanide: A comparative study. Appl Catal A:Gen. 2008;340(1):16-24.
[53] Islam SM, Roy AS, Mondal P, Mubarak M, Mondal S, Hossain D, et al. Synthesis, catalytic oxidation and antimicrobial activity of copper(II) Schiff base complex. J Mol Catal A:Chem. 2011;336(1-2):106-14.
[54] Cao TT, Zou CQ, Luo GF, Chen DX, Zhao XR, Li RP, et al. Heterogenous degradation of toxic organic pollutants by hydrophobic iron(III) schiff base complex under visible irradiation. Chem J Chinese U. 2011;32(1):105-12.
[55] Riva S. Laccases: blue enzymes for green chemistry. Trends Biotechnol. 2006;24(5):219-26.
[56] Suarez-Ojeda ME, Stuber F, Fortuny A, Fabregat A, Carrera J, Font J. Catalytic wet air oxidation of substituted phenols using activated carbon as catalyst. Appl Catal B:Environ. 2005;58(1-2):105-14.
[57] Louloudi M, Mitopoulou K, Evaggelou E, Deligiannakis Y, Hadjiliadis N. Homogeneous and heterogenized copper(II) complexes as catechol oxidation catalysts. J Mol Catal A:Chem. 2003;198(1-2):231-40.
[58] Santos A, Yustos P, Quintanilla A, Ruiz G, Garcia-Ochoa F. Study of the copper leaching in the wet oxidation of phenol with CuO-based catalysts: Causes and effects. Appl Catal B:Environ. 2005;61(3-4):323-33.